Journal of the Serbian Chemical Society
JSCS@tmf.bg.ac.rs • www.shd.org.rs/JSCS
J. Serb. Chem. Soc. *86* (11) 1089–1102 (2021)
JSCS–5485
Original scientific paper
Published 8 September 2021

LabVIEW virtual instrument for zone penetration studies in flow-based analytical systems

ALEKSANDRA KULJANIN and NATAŠA GROS*

University of Ljubljana, Faculty of Chemistry and Chemical technology, Večna pot 113, 1000 Ljubljana, Slovenia

(Received 9 July, revised 30 July, accepted 4 August 2021)

Abstract: In the flow method development, zone penetration studies are usually conducted as a part of the initial screening phase. A lack of an appropriate tool can keep these studies on the level of rough estimations. The developed LabVIEW virtual instrument (VI) which processes peak signals and calculates the overlapping area and fundamental peak-related parameters was used for the calculations in experiments that are modelling sample and reagent plug interaction within liquid conduits. The reliability of the predictions was initially confirmed on the artificial data set based on thirty-six files covering all the different types of cases that can be foreseen. To continue, the volumes of model solutions, propelling flow rate, and the coil length in the sequential injection analysis system, were varied by following the Box–Behnken response surface design. In three examples, it is demonstrated how the VI can help the planning of further experiments in the range which ensures the efficient zone overlapping, the economic exploitation of reagent plug and the adequate dispersion. The application of the VI is not limited just to the flow-based chemistry, it can also be used in spectroscopy and chromatography. In order to use the graphical user interface, it is not necessary to have the LabVIEW program installed.

Keywords: peak processing; peak overlapping area; open-code program; sequential injection analysis; dispersion coefficient.

INTRODUCTION

The processing and the analysis of peak signals are inevitable in many scientific disciplines. Different methods for peak evaluation have been developed and applied so far, depending on the problem which has to be solved.[1–8] The extracting information about the individual chemical component from the overlapped peak signals is still challenging in chromatographic analysis. Power functions were tested for the modulation of peak shape, noise decreasing[1,2] and for

* Corresponding author. E-mail: Natasa.Gros@fkkt.uni-lj.si
https://doi.org/10.2298/JSC210709058K

resolving partially overlapped peaks.[3] Deconvolution in gas chromatography was done by using an exponentially modified Gaussian model,[4] while multivariate curve resolution was employed for the resolving of overlapped HPLC peaks.[5] Methods founded on Gaussian model were used for the resolving of overlapped peaks in UV–Vis spectrum[6] and the deconvolution of peaks in chiral chromatography.[7] The flow analysis methods, as flow injection analysis (FIA), sequential injection analysis (SIA) and lab-on-a-valve (LOV), provide information about the analyte in the form of peak signal, too.[9] Unlike the aforementioned examples, where the peak overlapping was considered to be the unwanted phenomena, the investigation of zone penetration in flow systems means the evaluation of peak overlapping areas. Overlapping of the zones influences the reaction yield and the sensitivity of the method. The most common approach is to simulate a sample plug with a defined volume of a non-reactive dye, while the reagent plug is simulated with water or an adequate buffer, and *vice versa.* The overlapping area of recorded peaks gives information about the zone penetration and merging. Ružička and Hansen have reported that it is rather complex to create a general model for the prediction of peak profiles based on variations of different factors within the FIA system.[10] This is in agreement with the reported data dealing with the topic, where it was also underlined that the results obtained from the examinations of FIA systems cannot be extrapolated to other flow systems.[9] It was stated that the zone penetration and the dispersion are the key parameters for the successful performance of SIA systems.[11,12] The zone penetration studies were used for the investigation of the effects of a single bead string reactor on dispersion and mixing of the zones in the SIA system.[13] This type of studies was also conducted by Jakmunee and co-workers, in order to define optimal volumes and aspiration sequence for the examination of fruit juices acidity.[14] In the flow method development, the zone penetration is usually employed in the initial screening phase, and the changes in the overlapping area are judged by appearance.[15–17] Even if the numerical values were given, it was not exposed which approach was employed for zone penetration evaluation. Most common approach used in development of sequential injection and flow analysis methods is still univariate optimization.[18–20] More detailed study of the zone penetration and other parameters of importance could decrease the number of experiments in later phases. When programs of wider scope are used, it is necessary to adapt their functions to a specific application, which can be time-consuming and demanding. Also, the creation of automation scripts for general-purpose programs requires programming skills. The processes within Origin can be automatized by using LabTalk, scripting language native to Origin, or Origin C, high level programming language. Origin C provides the access to the import and export of data, processing, and analysis.[21] In Excel, the automation is usually done by employing Visual Basic.[22,23] National Instruments Laboratory Virtual Instrument Engineering

Workbench (NI LabVIEW) is a highly modular graphical programming language that disposes of large libraries of different functions, enables building adaptable instrumental platforms and convenient user interfaces.[24,25] The use of the LabVIEW VI for the processing and the chemometric analysis of spectroscopic data was demonstrated for modelling of the diffuse reflectance spectra in the visible, NIR and mid-IR spectra for the predictions of the mineral-organic composition of soil mixes.[26] The program was also utilized for creation of flexible platforms which facilitate employing and testing of different temperature and pressure sensors.[27,28] LabVIEW VIs were also applied for the precise control and the monitoring of hardware components of automated SIA systems.[29–31] However, to the best of our knowledge, the open code LabVIEW software for the zone penetration studies was not yet reported. Our main objective was to develop LabVIEW VI that would not only provide the user with the most fundamental peak-related parameters but it would also support the zone penetration studies in flow-based analytical systems, by the evaluation of the peak overlapping areas. To use the developed VI and its graphical user interface one does not have to be familiar with LabVIEW and it is not necessary to have the program installed. A further objective was to test the reliability of the predictions using artificial and experimental data sets and to demonstrate the usability of the VI for more comprehensive zone penetration studies of SIA system.

EXPERIMENTAL

Algorithm of the developed program

The algorithm of the developed program is presented in Fig. 1.

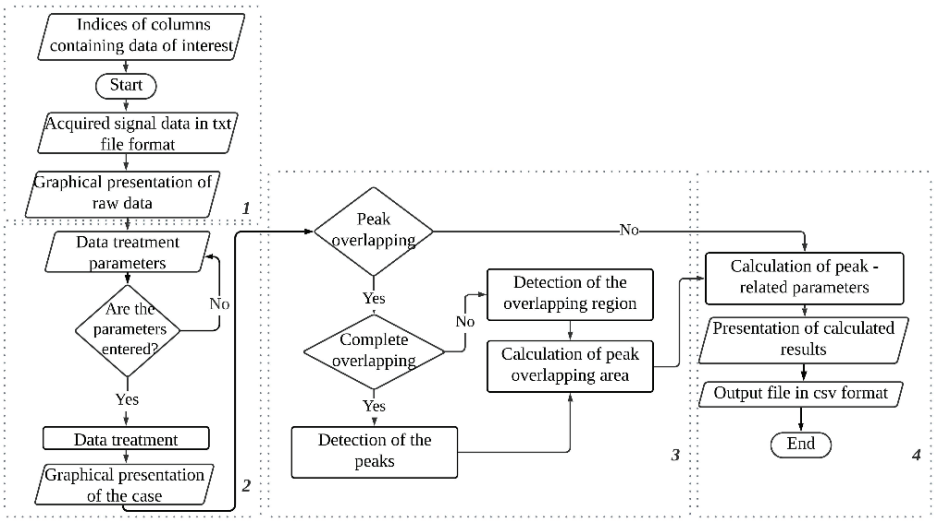

Fig. 1. Algorithm of the processes executed within four main sequence structures of the developed VI.

The program comprises four main sequence structures, and each of them executes a set of different operations. The graphical user interface is presented in Fig. 2.

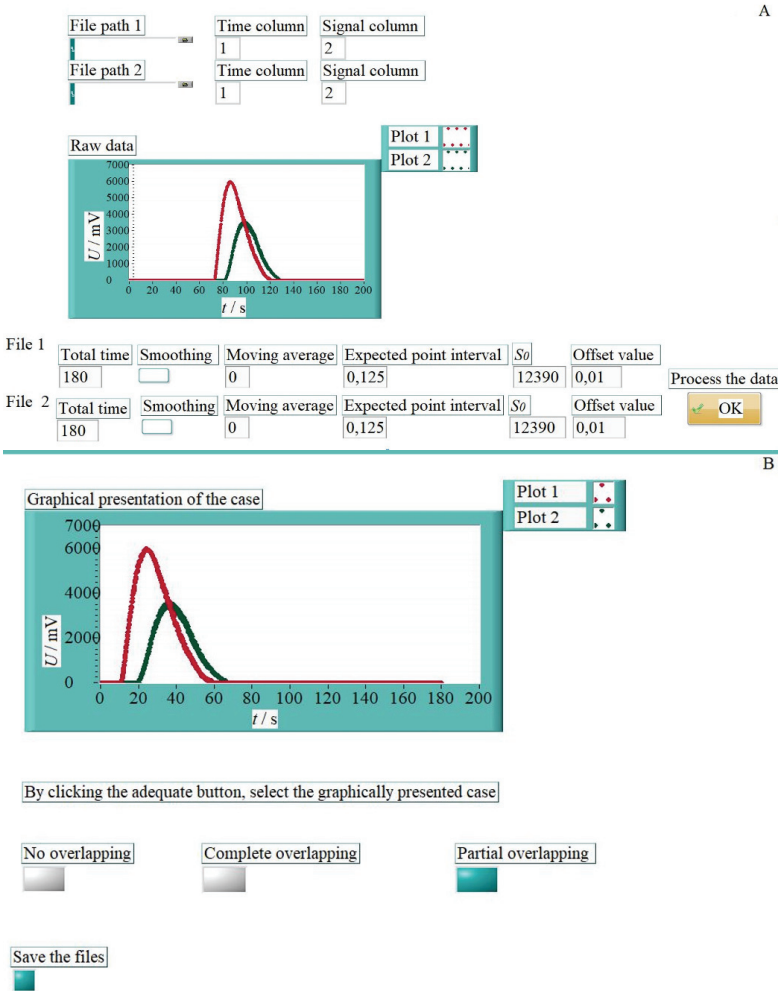

Fig. 2. The graphical user interface of the VI. Required input parameters and raw data presentation (A); graphical presentation of the processed data and choice of the case (B).

The numerical controls called the Time column and Signal column define which columns will be extracted from the raw data file, and it is necessary to fill them in before the program is started. After the program has been run, the user is offered to upload two text files of interest. The input data for the program has to be in the form of a text file with string headers on top and numerical data placed in columns. The number of columns is not limited, but at least one of them must have the header “Time” where the time is written. The read delimited spreadsheet VI has been used for file reading. A combination of functions and

subVIs from the Array and String palette has been used for data extraction. The last operation, executed within the first structure, is a graphical presentation of the raw data sets.

The next step is to define the following input parameters by filling in control fields: the total time interval, the expected point-to-point interval, the offset value, and the parameter S_0. If it is necessary, the user can also request the curve smoothing via moving an average function, by defining the number of points that will be used for the mean calculation. This structure is based on the do/while loop, and it operates until the value of the control button "Process the data" is set to true. The program waits for the input on the parameter values and does not execute other processes until it is done. From the moment when the data acquisition ended, the start of the relevant data acquisition is calculated based on the total time interval parameter. It is useful when data acquisition has been started in advance since it eliminates the initial part of the sequence of no value for further analysis. After that, the time axis is transferred to a relative. During the data acquisition, some points could have been missed due to computer's multitasking, especially if the point intervals are narrow. The problem was observed within the experimental data sets with 0.125 s data collection interval. The value of the expected point-to-point interval presents the input for the Interpolate 1 D VI, which was applied for the interpolation. In our case, the linear interpolation was satisfying since the number of points which defined the shape of the peak was high, and the signal interval was narrow.

The last parameter (S_0) presents the signal recorded when the detection cell is filled with undiluted solution, and it is used for the calculation of the dispersion coefficient. The demonstration of the effect of the processing tool on the acquired data sets is given in Fig. 3.

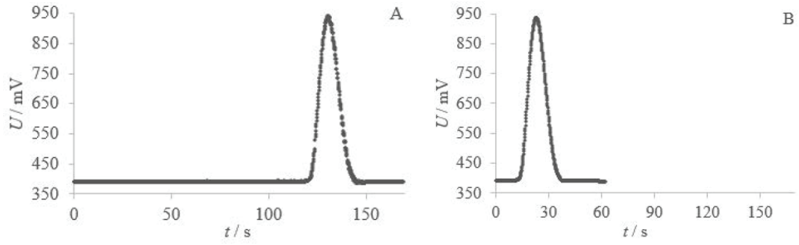

Fig. 3. Graphical presentation of the acquired data before (A) and after (B) the application of the processing tool.

The numerical detection of the intersection point is based on the minimal difference between two signals from different arrays, so it is necessary to have arrays of the same length. If not, the shorter array is recognized, and it is prolonged with its last element. The last process executed within the second sequence structure is the data presentation.

The presented sample and the reagent peaks give insight into what is happening within the liquid conduits. In general, it is possible to have three different situations. The graphical presentation of the cases is given in Fig. 4.

The third sequence structure contains an event structure. Based on the visualized data, the user decides between three possible events by choosing one of the options on the graphical interface: no overlapping (1), complete overlapping (2) or partial overlapping (3). Within all the events, the first step is the elimination of the signals below the offset value.

Event 1. Since the peaks do not overlap, this event just transfers the information that the overlapping area is zero to the next sequence structure.

Event 2. The program detects the narrower peak. The area of the smaller and narrower peak presents the overlapping area.

Event 3. The program detects the start and the end of the peaks. Later on, the signal columns from both arrays are extracted, subtracted, and the new 1D array is formed. The sign change within the 1D array indicates that the curves intersected. Depending on the number of the intersection points, one or two, the overlapping area is the sum of two or three sections.

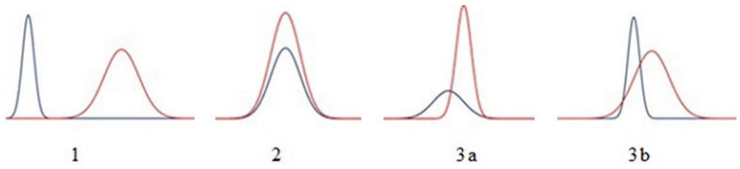

Fig. 4. Graphical presentation of the foreseen cases used as the basis for creation of simulation files (1 – no overlapping; 2 – total overlapping; 3a – partial overlapping with curves intersecting at one point; 3b – partial overlapping with curves intersecting at two points).

The user can also activate the control button "Save the files". The value of the local variable for the control is sent to the fourth structure.

The fourth structure employs the functions from Array, Comparison and Mathematical palette, and executes the calculation of individual peak areas, and the zone overlapping expressed as a fraction of total peaks area. Also, the other important peak-related parameters as dispersion coefficient, residence time, peak width, and peak height are calculated. If the value of the "Save the files" button was changed, the output CSV file composed of the processed data sets is exported. Afterward, the value of all control buttons is reset to false, and the program is prepared for the next run. Reliability of the software predictions was tested by weighing method. The results obtained by weighing correlate with VI predictions at a high level (R^2 = 0.9993). More details can be found in the Supplementary material to this paper.

Chemicals

Potassium chloride *p.a.* (Honeywell – Fluka, Germany) and milliQ water (Millipore SA, France) were used in the zone penetration studies. We have simulated the plug of the reagent with 0.15 mol L^{-1} potassium chloride, while the sample plug was simulated with milliQ water, and *vice versa*.

SIA system

A schematic presentation of the used SIA system is given in Fig. 5.

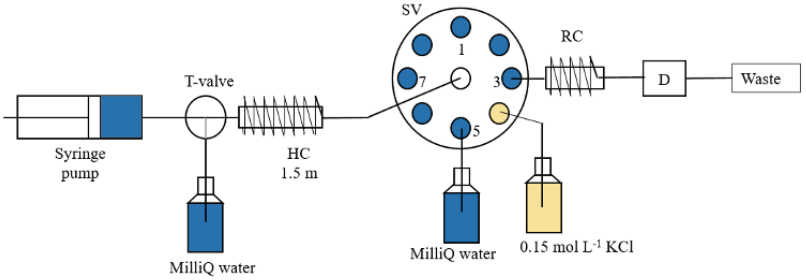

Fig. 5. Schematic presentation of the SIA system used for the experiments.

The system consisted of a Harvard Apparatus 11-Elite syringe pump, solenoid T-valve (Neptune Research, Inc., West Caldwell, NJ, USA), eight to one port selector valve (Vici Valco, Schenkon, Switzerland). Polytetrafluoroethylene tubings (internal diameter, i.d., 0.75 mm) obtained from Vici Valco, Switzerland, were used for the creation of holding coil (HC) and reaction coils (RC). A laboratory-made conductivity meter with stainless steel flow-through cell was used as a detector (D).

Zone penetration experiments

It is recognized that sample volume, reagent volume, propelling flow rate, and coil length are the factors which influence the yield of reactions performed within the flow systems. The important factors in the SIA system were varied in order to examine how they affect the most important parameter in sequential injection systems, the zone penetration. Box-Behnken response surface design in 12 blocks was used. The experimental matrix consisted of 27 experiments. Every measurement was conducted in four replicates. Four factors were varied at three levels, by respecting the rules of Box Behnken design, which is presented in Table I.

TABLE I. Experimental factors and factor levels chosen for the Box Behnken response surface design

Experimental factor	Level –1	Level 0	Level +1
Sample volume, μL	30	75	120
Reagent volume, μL	30	75	120
Propelling flow rate, $mL \cdot min^{-1}$	0.5	1	1.5
Coil length, cm	20	40	60

The reagent plug was simulated with 0.15 mol L^{-1} potassium chloride, while the sample plug was simulated with milliQ water, and *vice versa*. The sample plug was aspirated first, and subsequently the reagent plug. The aspiration flow rate was kept at constant 0.25 mL min^{-1} while the flow rate used for syringe refill was always 1 mL min^{-1}. The operating sequences of the SIA methods are presented in Table II. The obtained peaks were further processed and analyzed by the developed VI.

TABLE II. Operating sequences of used SIA methods

Step	Time, s	Pump	T-valve	Selector valve	Description
1	2	Stop	On	4	Switching the valve
2	7.2, 18 or 28.8	Reverse	On	4	Aspiration of KCl solution
3	2	Stop	On	5	Switching the valve
4	7.2; 18 or 28.8	Reverse	On	5	Aspiration of milliQ water
5	2	Stop	On	3	Switching the valve
6	45, 60 or 120	Forward	On	3	Propelling the plugs to the detector
7	2	Stop	Off	3	Switching T-valve
8	60	Reverse	Off	3	Filling in the syringe with milliQ water

The response surface graphs which present the influence of varied factors on the chosen responses were created. The chosen responses were: zone overlapping, dispersion coefficient of sample plug, dispersion coefficient of reagent plug and overlapped fraction of the reagent peak.

Software packages

The hardware control and the data acquisition were done *via* LabVIEW 2015 SP1 software, National Instruments, USA. For the design of the experiments and graphical presentation of the results in the form of response surface graphs, the Statgraphics Centurion (Statgraphics Technologies, Inc, USA) was used. For the creation of the scheme of developed VI, the Lucidchart application was applied.

RESULTS AND DISCUSSION

Benefits of more comprehensive studies of zone penetration in association with other peak-related parameters supported by the developed VI

As aforementioned, the zone penetration studies are usually a brief introductory step in flow method development. The geometry of every SIA system has specific characteristics, and it is profitable to explore how the change of important factors affects the response. A deeper understanding of the behaviour of liquid conduits can reduce the number of later experiments and contribute to greener analytical chemistry. A lack of an appropriate tool can keep these studies on the level of rough estimations, based on the judgments of peak overlapping by appearance. It is demonstrated here how the designed VI supports more comprehensive studies of zone penetration in association with other peak-related parameters. The conclusions in the continuation are derived from the three-level Box–Behnken design and presented as response surface graphs.

Zone penetration studies

For the introductory understanding of the behaviour of liquid conduits in the SIA system the overlapping area relatively expressed as a fraction of the total area of the two peaks, called the zone overlapping was used. The zone overlapping as a function of the sample and reagent volume for the flow rate 1 mL min^{-1} and 40 cm coil is presented in Fig. 6.

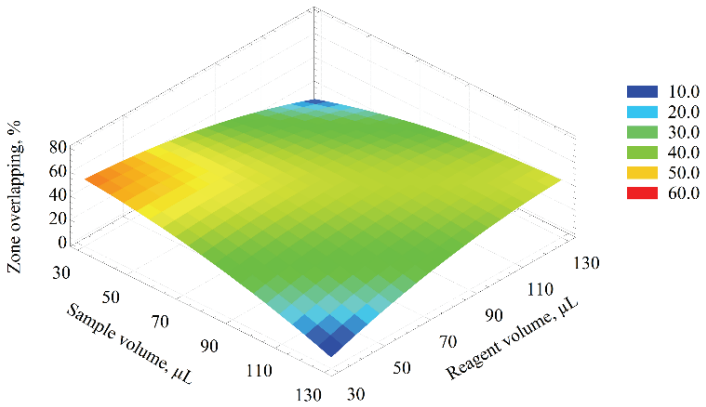

Fig. 6. The effect of sample and reagent volumes on zone overlapping at 1 mL min^{-1} flow rate and 40 cm coil length.

The combination of very low sample and reagent volumes (30–50 μL) resulted in the most efficient overlapping and zone penetration. In contrary to this, the lowest value of zone overlapping was obtained when low reagent volumes were combined with high sample volumes and *vice versa*. Low volume plugs overlap very efficiently, but it can be expected that they will be dispersed to a higher extent on their way to the detector. Low sample and reagent volumes can be considered for the development of analytical methods based on fast one-step reactions in combination with a detector of appropriate sensitivity. In that case, a manifold can employ a short reaction coil, and the effect of dispersion will consequently be less expressed.

Dispersion

The dispersion coefficients for reagent (D_r) and sample plug (D_s) were calculated as the VI's output parameters by dividing the signal recorded for 0.15 mol L^{-1} potassium chloride (S_0) by peak height. The obtained values were used for the creation of response surface graphs presented in Fig. 7.

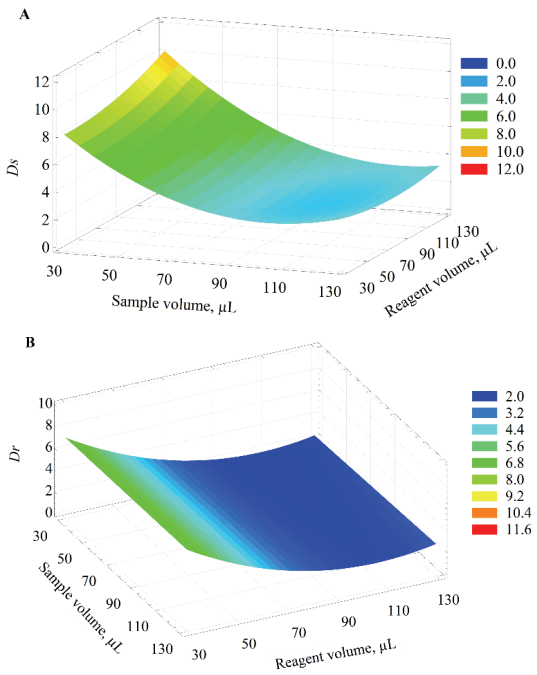

Fig. 7. The effect of sample and reagent volumes on sample dispersion coefficient (A) and reagent dispersion coefficient (B) at 1 mL min^{-1} flow rate and 40 cm coil length.

SIA systems employ bi-directional pumps for the manipulation of liquid plugs back and forth. The unique characteristic of SIA is that flow reversals are favouring the mutual interdispersion of reagent and sample, the reactants. The previous studies have shown that the first flow reversal is increasing the mixing of the zones significantly, while later cycles less affect the zone interpenetration.[11]

We confirmed that sample dispersion coefficients are higher compared to reagent dispersion coefficients. Since the sample plug is aspirated first, its dispersion is additionally affected as the sample plug is displaced and partially penetrated by the reagent plug. The flow reversal enhances interpenetration in the opposite direction. The sample dispersion coefficient varies between 2 and 10, over the tested range. The reagent dispersion coefficient exceeded value 3 only when low reagent volumes were used. It varies less over the tested range as the traveling path is shorter, and the sample volume has no effect on it. Even though the medium dispersion of a sample and a reagent plug is the most common, the model indicates that over the whole examined range dispersion coefficients are convenient and adaptable to the specific needs, considering the sample and reagent characteristics and the reaction type.

From the presented results, we can observe how the single flow reversal increased the dispersion of sample plug. In order to better evaluate the flow reversal effect on plug dispersion, the cell can be placed between the selector valve and the holding coil.

Zone penetration and reagent economy

In the very wide range of conducted experiments excluding the above mentioned combinations, the zone overlapping values were around 40 % (Fig. 7). Similar zone overlapping expressed relatively, corresponds to different overlapping areas, if presented in the units of measurement. Consequently, in the case of a definite reaction, a higher or lower quantity of a product would have been formed, respectively. By choosing the appropriate conditions one can adapt the signal to the sensitivity and the linear range of the detector. But, here an another aspect, the reagent economy was targeted, and it also cannot be judged based on the zone overlapping, since it considers the entire area of the two peaks. This is enabled by the VI which also provides the overlapped fraction of the reagent peak. The area of similar zone penetration profiles in the range of different volumes of sample and reagent plug was further explored, by considering under which combination of experimental conditions the reagent could have been more economically used, while keeping the zone overlapping value constant. Graph of the created contour plots in which the zone overlapping and the overlapped fraction of the reagent peak were used as responses and superimposed is presented in Fig. 8.

The scaling of the axis was the same for both graphs, and they were of the same size. The overlapped fraction of the reagent peak varied from 10 (pale blue area) to 100 % (dark blue area) over a range of different experimental values. When the overlapped fraction of the reagent peak reaches 100 %, the reagent peak is completely overlapped, and every part of the plug will participate in a chemical reaction. The other contour plot, describing the distribution of zone

overlapping values, was presented with grey lines with numbers adjoined. The zone overlapping, as a parameter, gives information concerning both plugs. By the overlaying of two response variables, an insight in the reagent economy, which is a very important aspect of SIA optimization was obtained. It was demonstrated on three examples how the VI can support more detailed zone penetration studies that help us plan the experiments in the range which ensures efficient zone overlapping, adequate dispersion, and high reagent exploitation. Some additional considerations are still possible.

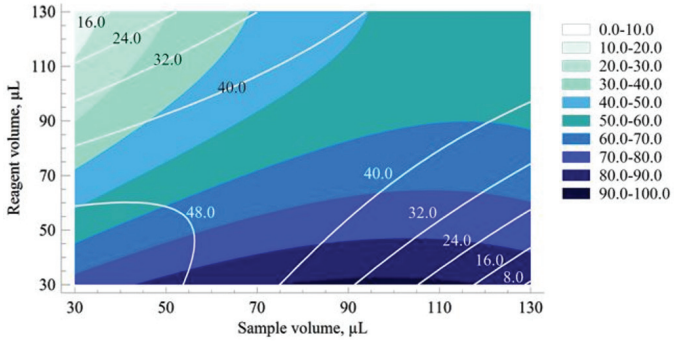

Fig. 8. Contour plots obtained when zone overlapping (grey lines) and overlapped fraction of the reagent peak (graded blue colour areas) were used as responses at 1 mL min^{-1} flow rate and 40 cm coil length.

CONCLUSION

The applicability of the created virtual instrument for the data pre-treatment, calculation of peak overlapping area, and the most important peak-related parameters was confirmed. The virtual instrument was applied to characterize the behaviour of the sample and reagent plug in a system with 0.75 mm i.d. tubes, 1 m holding coil, and 40 cm reaction coil at 1 mL·min^{-1} propelling flow rate. A general model was based on potassium chloride and conductometric detection. More detailed zone penetration studies, supported by the developed VI, enabled the general characterization of the behaviour of the SIA system. The presented studies supported with the experimental design techniques have also proven useful for the more specific goals. It was possible to detect the volume range of interest for two very important aspects in SIA method optimization, the reagent economy and the employment of detectors of different sensitivity. Even though the VI was developed for the processing of peak signals obtained within the flow system, its use is not only limited to this type of chemical analysis. The VI has the potential to be applied in other areas, *e. g.*, spectroscopy or chromatography. The examinations of the Stokes shift in fluorescence,[32,33] or the development of an expert system for simultaneous ion-chromatographic determination of ions in wide concentration range as found in highly mineralized waters,[34] are the

examples of studies that can also potentially profit from the VI. The developed software is available upon request from the authors. For the access to the graphical user interface of the created VI, it is not necessary to have the LabVIEW program installed. NI Run-Time engine 2015 SP1 which is required for running the executables created within the LabVIEW program, can be downloaded for free.[35] The more experienced users, already using the LabVIEW program, can further modify the code and adapt it to their specific needs.

SUPPLEMENTARY MATERIAL

Additional data and information are available electronically at the pages of journal website: https://www.shd-pub.org.rs/index.php/JSCS/article/view/10940, or from the corresponding author on request.

Acknowledgement. The financial support is gratefully acknowledged from the Slovenian Research Agency (ARRS) through program P1-0153.

ИЗВОД

LABVIEW ВИРТУЕЛНИ ИНСТРУМЕНТ ЗА СТУДИЈЕ ПРЕКЛАПАЊА ЗОНА У ПРОТОЧНИМ АНАЛИТИЧКИМ СИСТЕМИМА

ALEKSANDRA KULJANIN и NATAŠA GROS

University of Ljubljana, Faculty of Chemistry and Chemical technology, Večna pot 113, 1000 Ljubljana, Slovenia

Један од основних корака у развоју проточних метода је испитивање ефикасности преклапања зоне узорка и реагенса. Иако студије имају далеко већи потенцијал, евалуација параметара од значаја није довољно детаљна и користи се искључиво у почетним фазама истраживања. Креирани виртуални инструмент у LabVIEW програмском пакету омогућава обраду сигнала у форми пика, израчунавање површине преклапања зона као и осталих параметара у експериментима који моделују интеракцију зоне узорка и реагенса. Поузданост инструмента најпре је потврђена на сету од 36 фајлова који је креиран тако да обухвата све потенцијалне могућности за интеракцију зона у проточном систему. У наставку, поштујући правила Box–Behnken дизајна, вариране су запремине узорка и реагенса, брзина протока и дужина петље за мешање у секвенцијалном инјекционом систему. На три примера демонстрирано је како развијени виртуелни инструмент може бити користан при планирању експеримената у опсегу који ће омогућити ефикасно преклапање зона, економичну употребу реагенса и адекватну дисперзију зона. Употреба виртуелног инструмента није ограничена само на проточне системе, може наћи своју примену и у спектроскопији и хроматографији. Приступ графичком интефејсу могућ је и без претходне инсталације LabVIEW програма.

(Примљено 9. јула, ревидирано 30. јула, прихваћено 4. августа 2021)

REFERENCES

1. P. K. Dasgupta, Y. Chen, C.A. Serrano, G. Guiochon, H. Liu, J.N. Fairchild, R.A. Shalliker, *Anal. Chem.* **82** (2010) 10143 (https://doi.org/10.1021/ac102242t)
2. I. A. Haidar Ahmad, A. Blasko, J. Tam, N. Variankaval, H. M. Halsey, R. Hartman, E. L. Regalado, *J. Chromatogr., A* **1603** (2019) 1 (https://doi.org/10.1016/j.chroma.2019.04.017)

3. M. F. Wahab, A. Berthod, D. W. Armstrong, *J. Sep. Sci.* **42** (2019) 3604 (https://doi.org/10.1002/jssc.201900799)
4. H. Kong, F. Ye, X. Lu, L. Guo, J. Tian, G. Xu, *J. Chromatogr., A* **1086** (2005) 160 (https://doi.org/10.1016/j.chroma.2005.05.103)
5. M. J. Rodríguez-Cuesta, R. Boqué, F. X. Rius, J. L. Martínez Vidal, A. Garrido Frenich, *Chemometr. Intell. Lab. Systems* **77** (2005) 251 (https://doi.org/10.1016/j.chemolab.2004.09.010)
6. Y. Hu, J. Liu, W. Li, *Anal. Chim. Acta* **538** (2005) 383 (https://doi.org/10.1016/j.aca.2005.02.024
7. M. Perez-Baeza, L. Escuder-Gilabert, M. J. Medina-Hernandez, J. J. Baeza-Baeza, M. C. Garcia-Alvarez-Coque, *J. Chromatogr., A* **1625** (2020) 461273 (https://doi.org/10.1016/j.chroma.2020.461273)
8. M. Karakaplan, F. M. Avcu, *J. Chemom.* **34** (2020) 3229 (https://doi.org/10.1002/cem.3229)
9. V. Cerdà, L. Ferrer, J. Avivar, A. Cerdà, *Evolution and Description of the Principal Flow Techniques In Flow Analysis*, Elsevier, Boston, MA, 2014, pp. 1–42 (https://doi.org/10.1016/B978-0-444-59596-6.00001-2)
10. J. Ruzicka, E. H. Hansen, *Flow injection analysis*, John Wiley and Cons, New York, 1988, pp. 365–371 (ISBN: 978-0-471-81355-2)
11. T. Gubeli, G. D. Christian, J. Ruzicka, *Anal. Chem.* **63** (1991) 2407 (https://doi.org/10.1021/ac00021a005)
12. R. E. Taljaard, J. F. van Staden, *Lab. Rob. Autom.* **10** (1998) 325 (https://doi.org/10.1002/(SICI)1098-2728(1998)10:6<325::AID-LRA3>3.0.CO;2-L)
13. J. F. van Staden, T. McCormack, *Instrum. Sci. Technol.* **27** (1999) 167 (https://doi.org/10.1080/10739149908085847)
14. J. Jakmunee, T. Rujiralai, K. Grudpan, *Anal. Sci.* **22** (2006) 157 (https://doi.org/10.2116/analsci.22.157)
15. C. X. Galhardo, J. C. Masini, *Anal. Chim. Acta* **417** (2000) 191 (https://doi.org/10.1016/S0003-2670(00)00933-8)
16. W. Khongpet, S. Pencharee, C. Puangpila, S. Kradtap Hartwell, S. Lapanantnoppakhun, J. Jakmunee, *Talanta* **177** (2018) 77 (https://doi.org/10.1016/j.talanta.2017.09.018)
17. A. R. Araujo, M. L. Saraiva, J. L. Lima, *Talanta* **74** (2008) 1511 (https://doi.org/10.1016/j.talanta.2007.09.028)
18. L. D. Chen, J. Xu, T. Wang, Y. M. Huang, D. X. Yuan, Z. B. Gong, *Talanta* **232** (2021) 122404 (https://doi.org/10.1016/j.talanta.2021.122404)
19. S. Liawruangrath, K. Prasertboonyai, *Anal. Lett.* **54** (2021) 364 (https://doi.org/10.1080/00032719.2020.1764970)
20. T. J. Trinklein, M. Thapa, L. A. Lanphere, J. A. Frost, S. M. Koresch, J. H. Aldstadt, *Talanta* **231** (2021) 122355 (https://doi.org/10.1016/j.talanta.2021.122355)
21. *OriginLab*, https://www.originlab.com/index.aspx?go=PRODUCTS/Origin (accessed 31. 5. 2021)
22. J. Walkenbach, *Excel® 2010 Power Programming with VBA,* Wiley Publishing, Indianapolis, IN, 2010, pp. 1–10 (ISBN: 978-0-470-47535-5)
23. T. Mikhailova, S. M. Mustafina, V. Mikhailov, S. Mustafina, *Entomol. Appl. Sci. Lett.* **5** (2018) 21 (https://easletters.com/article/brwa-automation-of-controls-process-of-macro-of-microsoft-excel-file-for-data-processing-of-chemical-experiments)
24. L. Liu, J. Li, L. Deng, *Adv. Mat. Res.* **569** (2012) 808 (https://doi.org/10.4028/www.scientific.net/AMR.569.808)

25. *National Instruments*, http://www.ni.com (accessed 31.5.2021)
26. R. A. Viscarra Rossel, *Chemom. Intell. Lab. Systems* **90** (2008) 72 (https://doi.org/10.1016/j.chemolab.2007.06.006)
27. W.B. Wang, J. Li, Q. J. Wu, *J. Automat. Chem.* **2007** (2007) 68143 (https://doi.org/10.1155/2007/68143)
28. M. R. Liu, Y. Liu, Y, L. M. Zhou, *Micromachines* **12** (2021) 602 (https://doi.org/10.3390/mi12060602)
29. J. Ma, P. Li, Z. Chen, K. Lin, N. Chen, Y. Jiang, J. Chen, B. Huang, D. Yuan, *Anal. Chem.* **90** (2018) 6431 (https://doi.org/10.1021/acs.analchem.8b01490)
30. C. Lenehan, N. Barnett, S. Lewis, *J. Autom. Chem.* **24** (2002) 99 (10.1080/14639240210136747)
31. Y. Deng, P. C. Li, T. Y. Fang, Y. Y. Jiang, J. X. Chen, N. W. Chen, D. X. Yuan, J. Ma, *Anal. Chem.* **92** (2020) 4379 (10.1021/acs.analchem.9b05252)
32. X. L. Ronghui Zhou, Q. Yang, P. Wu, *Chin. Chem. Lett.* **30** (2019) 1843 (https://doi.org/10.1016/j.cclet.2019.07.062)
33. A. Bavali, P. Parvin, M. Tavassoli, M. R. Mohebbifar, *Appl. Opt.* **57** (2018) B32 (https://doi.org/10.1364/AO.57.000B32)
34. N. Gros, B. Gorenc, *J. Chromatogr., A* **697** (1995) 31 (https://doi.org/10.1016/0021-9673(95)92840-K)
35. *National Instruments LabVIEW*, https://www.ni.com/sl-si/support/downloads/software-products/download.labview-runtime.html#369481 (accessed 31. 5. 2021).